RND3/RhoE deficiency in preeclamptic women impairs placental mitochondrial function via regulation of the PPARgamma-UCP2 pathway

Xiaojing Yue[1 † *], Liping Huang[1 †], Yanlin Ma[2 †], Lu Chen[1], Jiang Chang[3], Mei Zhong[1], Zhijian Wang[1], Ying Sun[4], Xia Chen[1], Fei Sun[1], Lu Xiao[1], Jianing Chen[1], Yinjun Lai[1], Chuming Yan[1], Yanhong Yu[1 *]

1. Department of Obstetrics and Gynecology, Nanfang Hospital, Southern Medical University, Guangzhou, China.
2. Hainan Provincial Key Laboratory for Human Reproductive Medicine and Genetic Research, Reproductive Medical Center, The First Affiliated Hospital of Hainan Medical University, Hainan Medical University, Haikou, China
3. Institute of Biosciences and Technology, Texas A&M University Health Science Center, Houston, US.
4. Department of Obstetrics and Gynecology, Affiliated Shenzhen Maternity and Child Healthcare Hospital, Southern Medical University, Guangzhou, China

Running Title: Rnd3 regulates mitochondrial function in preeclampsia

***Correspondence to**: Yanhong Yu MD, PhD (yuyh1010@sina.com); Xiaojing Yue, PhD (yuexj1986@163.com);
Phone: (86) 020-62787551
Mailing address: Southern Medical University, 1023 South Shatai Rd, Guangzhou 510515, China.

†These authors contributed equally to this work.

Abstract

Preeclampsia (PE) is a life-threatening hypertensive disorder in pregnancy. Mitochondrial-mediated oxidative stress has been implicated in the etiology of PE with unknown underlying mechanism. We identified the downregulation of Rnd3 in the placental tissues and the primary trophoblasts from PE patients, associated with increased ROS generation and damaged mitochondrial integrity. Knockdown of Rnd3 in trophoblastic cells resulted in mitochondrial injury with membrane potential depolarization and proton leakage. Mechanistic studies indicated that Rnd3 stimulated the mitochondrial uncoupling protein 2 (UCP2) signaling, via its physical interaction with peroxisome proliferators-activated receptor γ (PPARγ). Rnd3 deficiency-mediated mitochondrial dysfunction was attenuated by overexpression of PPARγ. Finally, Rnd3 overexpression in human PE primary trophoblasts partially rescued the mitochondrial defect and oxidative stress. We conclude that Rnd3 acts as a novel protective factor in placental mitochondria through PPARγ-UCP2 signaling. Downregulation of Rnd3 in PE patients may explain the mitochondrial stress involved in the pathogenesis of PE.

Keywords: Small GTPase, Preeclampsia, Mitochondrion, Oxidative stress, PPARγ, UCP2

Preeclampsia (PE) is a pregnancy complication that occurs after the 20th gestational week and is characterized by maternal hypertension, proteinuria and multi-organ injuries. It affects 5-7% of pregnancies and is the leading cause of perinatal morbidity and mortality[1-3]. Although the mechanisms responsible for the pathogenesis of PE have not been entirely clarified, placental oxidative stress along with poor vascularization is thought to be its main cause[2, 4]. Oxidative stress is generated by the imbalance of reactive oxygen species (ROS) and the endogenous oxidant scavenging system[5]. It has been reported that ROS levels are increased during normal pregnancy due to low oxygen tension in early gestation[6, 7]. However, excessive ROS accumulation was identified in PE pathogenesis as the contributor to endothelial dysfunction and placental inflammation response[7-9]. Although shallow invasion of trophoblasts to decidua and subsequent failed spiral artery remodeling participate in placental ischemia and oxidative stress, accumulating evidence has shown that mitochondrial dysfunction during PE can induce an increase in the levels of ROS[10-12]. Altered morphology of mitochondria, including swelling and disappearance of cristae, has also been observed in trophoblasts of PE placentae[13]. However, a limited number of studies have investigated the molecular machinery of the mitochondrial ROS during PE.

peroxisome proliferators-activated receptor γ (PPARγ) is a ligand-inducible transcription factor that plays key roles in mitochondrial function, biogenesis, dynamics and metabolism[14, 15]. PPARγ has been implicated as an important regulator of placental vasculature and of the differentiation of complicated trophoblast lineages[16-18]. Loss of PPARγ in a mouse model caused embryonic lethality at D9.5-10.5 and the histological analysis indicated major placental defects[19]. Moreover, several recent studies revealed that the levels of the circulating agonists of PPARγ were increased in pregnancy, whereas they were significantly reduced in PE patients[19, 20]. Administration of rosiglitazone, a selective PPARγ agonist, could largely ameliorate PE in a RUPP-induced PE rat model[21], whereas it could also improve the survival of trophoblast cells by recovering the mitochondrial membrane potential and

reducing ROS generation[22]. This suggested that PPARγ may serve as a novel pharmacological target for PE. Nevertheless, the regulatory mechanism of the downregulated PPARγ signaling in PE remains unknown.

Rnd3 is a small GTPase, also called RhoE that exhibits multiple regulatory functions in carcinogenesis, cardiovascular diseases and neural development according to our recent studies[23-28]. *Rnd3* was proposed to be a PE candidate gene based on a population study. A specific *Rnd3* SNP (rs115015150) was associated with PE and several quantitative cardiovascular risk traits[29]. Subsequent research works illustrated that Rnd3 was involved with PE and regulating the proliferation, migration and invasion of trophoblast cells[30-32]. In the present study, the data indicated a novel protective function of Rnd3 for defective mitochondrial-induced placental oxidative stress. Rnd3 expression was downregulated in placentae from PE patients and this downregulation led to mitochondrial dysfunction and accumulated ROS in placental trophoblast cells. The molecular mechanism of Rnd3-mediated mitochondrial integrity was verified by experiments demonstrating the physical interaction of its protein with PPARγ and the stimulation of the PPARγ protein expression in nuclei. The uncoupling protein 2 (UCP2) was transcriptionally regulated by PPARγ and was involved in the regulation of mitochondrial membrane potential and ROS generation. The downregulated PPARγ-UCP2 cascade was identified in the placentae from PE patients and could be reversed by Rnd3 overexpression along with rescued mitochondrial dysfunction in human PE primary placental trophoblasts. The findings revealed a new function of this small GTPase in modulating the PPARγ-UCP2 pathway and provided a potential new target for therapeutic manipulation of PPARγ-UCP2 signaling.

Methods

Methods and associated references were available in detail in the Data Supplement of the article.

Statistical analysis

The data was expressed as the mean ± standard deviation (SD). An unpaired, two-tailed Student's *t* test was used for two-group comparison. The one-way ANOVA followed by the Student-Newman-Keuls method was used for multiple-group comparison. All analyses were conducted using GraphPad Prism 8.0. A value of $P<0.05$ was considered for significant difference.

Results

The expression of Rnd3 is downregulated in human placentae with PE

To investigate the role of Rnd3 in PE, its expression levels were measured in 24 human placentae from PE patients and 34 normal placentae. Women with a history of smoking and drinking or with a diagnosis of chronic hypertension or gestational diabetes mellitus were excluded from the present study. In the placentae with PE, a 62.9% decrease was noted in the RND3 protein levels (Fig.1A) and a 46.0% decrease was noted in the *Rnd3* mRNA level (Fig. 1B). This clinical observation suggested that Rnd3 may act as a potential regulator in the pathogenesis of PE.

RND3 protein expression is downregulated in human PE primary trophoblasts and is associated with severe oxidative stress and apoptosis

Oxidative stress is a main regulator of PE development. In the placental tissue sections, severe oxidative stress was noted in the human placentae with PE (Fig. 2A). Systemic experiments based on human primary trophoblasts (PTBs) were conducted for the understanding of the underlying mechanisms involved in this process. Human PTBs were isolated from normal term placentae and from placentae with a terminated pregnancy in the third trimester of PE patients. The PTBs were identified by immunostaining of the surface marker cytokeratin 7 (CK7) (Fig. 2B). The purity of the isolated PTBs was 97% according to nuclear counterstaining (Fig. 2B). The protein level of RND3 in the PTBs was detected by immunostaining analysis. Rnd3 was universally expressed in the cytoplasm and nuclei of the trophoblasts (Fig 2C). Reduced Rnd3 expression was associated with increased ROS accumulation and was

91 detected in the PE patient-derived PTBs (Fig 2C). To mimic the pathological PE
92 placental environment, hypoxic cell culture of PTBs was established. Following
93 induction of hypoxia, additional ROS accumulation and apoptosis were observed in
94 the PE PTBs compared with those noted in the control PTBs (Fig 2D). This suggested
95 that PE PTBs were more sensitive to hypoxic stress. Rnd3 may participate in the
96 development of PE via the regulation of ROS generation.
97

98 **Human PE primary placental trophoblasts are predisposed to mitochondrial**
99 **damage**

100 To explore the underlying mechanism of Rnd3-associated oxidative stress in PE,
101 trophoblastic mitochondria, which are the main source of ROS, were analyzed by
102 electron microscopy. In the ultrathin sections of the placental tissues, a borderline
103 between the layers of syncytiotrophoblast (STB) and cytotrophoblast (CTB) could be
104 clearly identified. In the CTB of the PE placentae, swelling mitochondria with loss of
105 cristae were observed, which were the typical characteristics of mitochondrial damage
106 (arrows pointed, Fig 3A). We further analyzed the mitochondrial membrane potential
107 in PTBs. Using JC1 staining, we compared the mitochondrial membrane potential
108 between the control PTBs and the PE PTBs with or without hypoxic stimuli. The
109 ratios of JC1 red/green fluorescence between the two groups indicated no difference
110 at the baseline (Fig 3B). The mitochondrial membrane potential was reduced in
111 response to hypoxic challenge. However, the red/green fluorescence emission ratio
112 was collapsed in PE PTBs compared with that noted in the control PTBs (Fig 3B),
113 indicating that PE PTBs were predisposed to hypoxia-induced mitochondrial injury.
114

115 **Overexpression of Rnd3 protects the trophoblastic cells from ROS generation**
116 **and induction of apoptosis**

117 To investigate the potential role of Rnd3 deficiency in inducing oxidative stress in PE
118 PTBs, we manipulated Rnd3 expression in the trophoblastic BeWo cell line. Hypoxic
119 cell culture was applied to induce ROS generation. ROS levels were determined by
120 DHE fluorescence labeling and the detection of cellular 8-isoprostane levels. The

121 GFP-Rnd3 expressing BeWo cells displayed significantly decreased ROS levels
122 compared with those of the surrounding non-GFP-Rnd3 cells (Fig 4A). Consistent
123 with these observations, myc-Rnd3 overexpression led to decreased 8-isoprostane
124 levels (Fig 4B) and ameliorated cell apoptosis (Fig 4C-D), indicating that Rnd3
125 modulated the production of ROS in trophoblasts. Rnd3 deficiency was observed in
126 human PE PTBs and may be the cause of severe oxidative stress and apoptosis in PE.
127

128 **Rnd3 deficiency leads to mitochondrial damage in BeWo trophoblastic cells**

129 To investigate if mitochondria contributed to Rnd3-mediated ROS generation, we
130 knocked down Rnd3 in BeWo cells. Electron microscopy of Rnd3 knockdown BeWo
131 cells revealed mitochondrial injury. The compromised mitochondria displayed a
132 structure with damaged cristae and swelling mass (arrow pointed, Fig 5A). Consistent
133 with the morphological changes, the mitochondrial transmembrane potential was also
134 depolarized following Rnd3 knockdown (Fig 5B). Subsequently, the effects of Rnd3
135 on mitochondrial function were assessed by measuring the oxygen consumption rate
136 (OCR) in different respiratory states. The comparison of the Rnd3 knockdown group
137 and the control group indicated no significant differences in the OCR of the basal
138 respiration, maximal respiration and space capacity (Fig 5C). However, a 2.4-fold
139 increase in the proton leak associated OCR was detected in the Rnd3 knockdown
140 BeWo cells (Fig 5C), indicating the uncoupling of ATP synthesis and substrate
141 oxidation. Consistent with this result, the mitochondrial coupling efficiency was
142 reduced in the siRnd3 group (Fig 5D).
143

144 **Rnd3 facilitates the protein accumulation of PPARγ and stimulates the**
145 **expression of UCP2 in trophoblasts**

146 To explore the underlying mechanisms of Rnd3-mediated mitochondrial dysfunction,
147 the mRNA expression levels of the mitochondrial regulatory factors and ROS
148 scavengers were evaluated in siRnd3 transiently transfected BeWo cells. The analysis
149 indicated no significant difference between siRnd3 and sicontrol groups with regard
150 to the mRNA levels of the transcription factors *PPARγ*, *PPARγ* coactivator 1-α

151 (*PGC1-α*), peroxisome proliferator-activated receptor α (*PPARα*), nuclear respiratory
152 factor 1 (*NRF1*), and mitochondrial transcription factor A (*TFAM*) (sFig 1). No
153 significant differences were also noted with regard to the levels of the endogenous
154 ROS scavengers superoxide dismutase 1 (SOD1) and superoxide dismutase 2 (SOD2)
155 (sFig 1).
156
157 Mitochondrial uncoupling protein 2 (UCP2) is critical for mitochondrial respiratory
158 coupling. Rnd3 promoted the protein and the mRNA expression levels of *UCP2*,
159 whereas knockdown of Rnd3 resulted in UCP2 deficiency (Fig 6A-6C), which was
160 consistent with the mitochondrial respiratory coupling defect in siRnd3-transfected
161 cells. As PPARγ has been identified as a transcriptional regulator of UCP2[33], we next
162 assessed its expression levels. It is interesting to note that although the mRNA
163 transcripts of PPARγ did not change following manipulation of *Rnd3* (sFig 2), the
164 PPARγ protein expression was stimulated by myc-Rnd3 overexpression and was
165 repressed by Rnd3 knockdown (Fig 6A-6B), suggesting a possible post-translational
166 regulation of PPARγ by Rnd3.
167
168 **RND3 is physically bound to PPARγ and results in the accumulation of PPARγ in**
169 **the nuclei**
170 To investigate if PPARγ protein could be functionally regulated by Rnd3, we knocked
171 down and overexpressed the latter in BeWo cell cultures. As a transcription factor, the
172 nuclear distribution of PPARγ is critical for maintaining its biological function. We
173 detected apparent nuclear accumulation of PPARγ protein corresponding to the
174 increase in Rnd3 expression. The opposite trend was observed when Rnd3 was
175 knocked down (Fig 6D). Subsequently, a luciferase experiment was conducted in
176 order to determine if Rnd3 caused any effect on its transcriptional activity. The
177 luciferase reporter was driven by a *UCP2* promoter, which was responsible for the
178 PPARγ-dependent transcriptional activity. Myc-Rnd3 overexpression resulted in a
179 5.2-fold increase in luciferase activity compared with that of the control, while
180 downregulation of Rnd3 weakened PPARγ transcriptional activity and resulted in

181 68% declined luciferase signal (Fig 6E). To further explore the potential mechanism
182 of Rnd3-induced PPARγ protein accumulation, we performed an *in vivo*
183 coimmunoprecipitation assay with 293T cells. As shown in Fig 6F, physical
184 interaction between Myc-RND3 and Flag-PPARγ proteins was detected. Moreover,
185 we performed co-immunostaining of these two proteins in BeWo cells and confirmed
186 the co-localization of RND3 and PPARγ protein molecules and the reduced nuclear
187 PPARγ protein levels in Rnd3 knockdown cells (Fig 6G).
188

189 **Mitochondrial dysfunction mediated by Rnd3 deficiency is attenuated by PPARγ**
190 **overexpression**

191 To assess whether PPARγ downregulation is responsible for Rnd3 deficiency-induced
192 mitochondrial defects, Flag-PPARγ was overexpressed in Rnd3 knockdown BeWo
193 cells. The improvement in mitochondrial membrane potential and mitochondrial
194 morphological integrity was observed following PPARγ overexpression (Fig 7A-C).
195 The ROS levels were detected by DHE labeling. We also detected 8-isopropane levels.
196 PPARγ overexpression further ameliorated Rnd3 deficiency-mediated oxidative stress
197 (Fig 7D-F). We analyzed the expression levels of UCP2 in Rnd3 knockdown BeWo
198 cells with or without administration of Flag-PPARγ. As expected, PPARγ attenuated
199 Rnd3 deficiency-induced UCP2 downregulation both at the mRNA and protein levels
200 (Fig 7G-H). Finally, we assessed the mitochondrial respiratory functions of the
201 different groups of BeWo cells. Overexpression of PPARγ significantly protected the
202 mitochondrial function with improved proton leakage and coupler efficiency (Fig
203 7I-J).
204

205 **Adenoviral-mediated Rnd3 overexpression in human PE primary trophoblasts**
206 **rescues oxidative stress and mitochondrial defect**

207 Rnd3 downregulation was demonstrated in human PE-PTBs along with severe
208 oxidative stress and mitochondrial injury. To further reveal the critical role of Rnd3 in
209 the clinical pathology of PE, we overexpressed hRnd3 in human PTBs by
210 adenoviral-mediated gene delivery. Elevated RND3 protein levels in Ad-GFP-hRnd3

211 treated PTBs were confirmed by western blot analysis (Fig 8D). In the absence of
212 Ad-GFP-hRnd3 infection, the baseline PE-PTBs exhibited higher ROS levels
213 compared with those of the control-PTBs (Fig 8A, cells displaying no GFP, pointed
214 by long arrows). Following infection with Ad-GFP-hRnd3, the ROS levels of the
215 PE-PTBs were significantly reduced (Fig 8A, cells displaying GFP, pointed by arrow
216 heads). The levels of 8-isopropane were decreased in PE-PTBs following
217 Ad-GFP-hRnd3 application (Fig 8B), which was consistent with the previous
218 observations. Increased expression levels of PPARγ and UCP2 were observed, as
219 expected, in the PTBs with Ad-GFP-hRnd3 (Fig 8C-D). In addition to regulating the
220 PPARγ/UCP2 pathway, Rnd3 further attenuated the mitochondrial function in
221 PE-PTBs (Fig 8E-G).
222

223 **Downregulation of the expression levels of PPARγ and UCP2 were observed in**
224 **human placentae with PE**

225 The expression levels of PPARγ and UCP2 were evaluated in human PE placental
226 tissues. The experiments aimed to offer additional insight in the clinical relevance of
227 the regulation of the PPARγ/UCP2 pathway by Rnd3 in PE. PPARγ protein levels
228 were downregulated in PE placentae. Consistent with the post-transcriptional
229 regulation of PPARγ by Rnd3, the corresponding mRNA levels of *PPARγ* indicated no
230 significant changes between the control and PE groups (Fig 9A-B). The mRNA
231 transcripts of *UCP2* and its protein levels were reduced in human PE placentae (Fig
232 9A and C).
233

234 **Discussion**

235 PE has been suggested as a mitochondrial disorder from the late 1980s[34]. The
236 mitochondrion is an important organelle that generates energy during pregnancy and
237 is important in regulating cellular metabolism[35]. A damaged mitochondrion is
238 characterized by disturbed electron transport chain (ETC) and is the source of ROS
239 formation that contributes to placental impairment. The leakage of the electrons from

240 the complexes Ⅰ and Ⅱ of the mitochondrial transport chain to the molecular
241 oxygen produces the reactive superoxide ion[8, 36]. Proteome analysis of PE placentae
242 has shown that the abnormal expression levels of the respiratory complex proteins
243 were associated with the generation of ROS in the mitochondrial respiratory chain[37].
244 Loss of mitochondrial control of ROS seems to trigger vascular inflammation and
245 endothelial dysfunction, which is characterized by the hyper-sensitivity to
246 vasoconstriction and low anticoagulant activity[38]. This process makes a significant
247 contribution to the pathogenesis of PE[39].
248
249 Increased RND3 protein expression has been reported in pregnant myometria
250 compared with myometrial samples from non-pregnant women. The roles of Rnd3 in
251 the myometrium have been implicated in regulating uterine quiescence and calcium
252 sensitization[40-42]. We compared the *Rnd3* mRNA levels in human villi at the first
253 trimester with the term placental tissues. An increase in *Rnd3* mRNA expression
254 levels was demonstrated during pregnancy (sFig3). The clinical significance of the
255 upregulation of Rnd3 in placental development remains unknown. Certain studies
256 have suggested the function of Rnd3 on placental trophoblasts. A research group
257 reported that the lncRNAs HOXA11-AS and TUG1 were downregulated in PE and
258 that the two lncRNAs could promote trophoblast proliferation and migration by
259 repressing Rnd3[30, 31]. In contrast to these observations, Rnd3 has also been proposed
260 as a stimulator of trophoblast cell invasion in PE, under the repression caused by
261 miR-182-5p[32]. However, the expression levels of Rnd3 in PE patients were not
262 detected in these studies.
263
264 In the present study, a critical role of Rnd3 was revealed with regard to the
265 pathogenesis of PE. A 62.9% reduction in RND3 protein levels and a 34.4% reduction
266 in *Rnd3* mRNA levels were detected in human PE placentae at the third trimester.
267 While the exact cause of Rnd3 downregulation in PE remains unknown, the
268 understanding of the pathological consequence of Rnd3 downregulation is important
269 and has considerable clinical significance.

It is interesting to note that the mitochondrial DNA (mtDNA) copy number is increased in human early-onset PE placentae compared with that of the normal control[12], suggesting the compensatory mitochondrial biogenesis in response to the insufficient energy supply. The data reported in the present study indicated that Rnd3 deficiency in trophoblast cells induced uncoupling in the ETC and electron leakage. Similar with the compensatory mitochondrial biogenesis in human PE placentae, the generation of mtDNA was stimulated in the situation of Rnd3 knockdown (sFig 2). The ultrastructural data further indicated the increased mitochondrial number, as determined by electron microscopy, in siRnd3 transfected BeWo cells (Fig5A). The findings suggested that mitochondrial biogenesis was boosted in trophoblasts in response to the Rnd3 insufficiency. However, the adaptive response failed to generate functional competent mitochondria as a result of the downregulation of the PPARγ/UCP2 pathway.

Uncoupling proteins (UCPs) are mitochondrial transporters in the inner membrane mediating dissipation of proton gradient. By uncoupling oxidative phosphorylation from ATP synthesis, UCPs play a critical role in controlling ROS production from mitochondrial ETC[43-45]. Out of the five UCP homologues, UCP2 is ubiquitously expressed in the heart, adipose tissue, skeletal muscle, kidney, lung and placenta as well as in immune cells[46]. UCP2 exerts protective properties against oxidative damage by reducing ROS generation via decreasing mitochondrial proton gradient and local oxygen availability[47]. Inhibition of UCP2 by GDP leads to a burst of the mitochondrial membrane potential and increased H_2O_2 levels in the spleen and thymus, which is followed by proton gradient collapse[48]. Moreover, deletion of the *UCP2* gene in mice exhibited persistent ROS accumulation and activated macrophage immunity[49,44]. UCP2 has also been reported as a protector of mitochondrial impairment. Knockdown of UCP2 in HK-2 cells and astrocytes resulted in increased apoptosis, oxidative stress and damaged mitochondrial ultrastructure and function[50, 51]. UCP2 deficiency induces elevation of mitochondrial membrane potential. This

300 process has been suggested as a trigger of mitochondrial injury. The long-lasting rise
301 of the mitochondrial membrane potential can induce the opening of the mitochondrial
302 permeability transition pore (mPTP), which non-selectively increases the exchange of
303 ions and solutes leading to the membrane potential depolarization, mitochondrial
304 matrix swelling and cell death[52, 53]. In the present study, Rnd3-mediated
305 downregulation of UCP2 in BeWo cells resulted in increased ROS production and
306 mitochondrial damaged phenotypes. These processes were accompanied by collapse
307 of membrane potential, abnormal ultrastructure, elevated proton leakage and low
308 coupling efficiency of ETC. The expression of Rnd3 in human primary PE trophoblast
309 could partially increase UCP2 expression and ameliorate the mitochondrial functional
310 defect. The findings indicated the role of UCP2 in mitochondrial ROS-mediated
311 etiology of PE development.
312
313 The transcriptional control proteins of UCP2 have been demonstrated with the
314 involvement of the peroxisome proliferator-activated receptors (PPARs)[54].
315 Thiazolidinedione is a PPAR agonist, which specifically activates PPARγ and has the
316 ability to increase *UCP2* gene expression in adipose tissues from rodents and human
317 patients[55, 56]. PPARγ and its ligands directly activate *UCP2* gene promoter in muscle
318 cells and adipocytes[54] via the E-box element proximal to the *UCP2* promoter[33]. In the
319 present study, downregulated PPARγ/UCP2 signaling was detected in human PE
320 placentae, contributing to mitochondrial defect and oxidative stress in PE primary
321 trophoblasts. However, the upregulation in the expression levels of PPARγ and UCP2
322 have also been reported in the pathological placentas of maternal nutrient restriction,
323 attributing to enhanced fatty acid metabolism and limited glucose utilization[57].
324 Therefore, the homeostasis of the PPARγ/UCP2 axis is critical in maintaining normal
325 placental function.
326
327 **Sources of Funding**
328 This study was supported by the following funding sources: the Major Science and
329 Technology Program of Hainan Province ZDKJ2017007 (Y. Ma), the National

Natural Science Foundation of China 81771609 (Y. Yu), 81601317 (X. Yue), and 81960283 (Y. Ma), the Natural Science Foundation of Guangdong Province 2017A030313584 and 2019A1515010290 (X. Yue), the Outstanding Youth Development Scheme of Nanfang Hospital Southern Medical University 2018J010 (X. Yue), the Special Fund for Cooperative Innovation and Platform Environment Construction 2015B050501006 (M. Zhong).

Disclosure

None.

340 **References**

341

342 1. Rana S, Lemoine E, Granger JP and Karumanchi SA. Preeclampsia: Pathophysiology,
343 Challenges, and Perspectives. *Circ Res*. 2019;124:1094-1112.
344 2. Steegers EA, von Dadelszen P, Duvekot JJ and Pijnenborg R. Pre-eclampsia. *Lancet*.
345 2010;376:631-44.
346 3. Khan KS, Wojdyla D, Say L, Gulmezoglu AM and Van Look PF. WHO analysis of causes of
347 maternal death: a systematic review. *Lancet*. 2006;367:1066-1074.
348 4. Hladunewich M, Karumanchi SA and Lafayette R. Pathophysiology of the clinical
349 manifestations of preeclampsia. *Clin J Am Soc Nephrol*. 2007;2:543-9.
350 5. Birben E, Sahiner UM, Sackesen C, Erzurum S and Kalayci O. Oxidative stress and antioxidant
351 defense. *World Allergy Organ J*. 2012;5:9-19.
352 6. Elliot MG. Oxidative stress and the evolutionary origins of preeclampsia. *J Reprod Immunol*.
353 2016;114:75-80.
354 7. San Juan-Reyes S, Gomez-Olivan LM, Islas-Flores H and Dublan-Garcia O. Oxidative stress
355 in pregnancy complicated by preeclampsia. *Arch Biochem Biophys*. 2020;681:108255.
356 8. Myatt L. Review: Reactive oxygen and nitrogen species and functional adaptation of the
357 placenta. *Placenta*. 2010;31 Suppl:S66-9.
358 9. Sanchez-Aranguren LC, Prada CE, Riano-Medina CE and Lopez M. Endothelial dysfunction
359 and preeclampsia: role of oxidative stress. *Front Physiol*. 2014;5:372.
360 10. Wang Y and Walsh SW. Placental mitochondria as a source of oxidative stress in
361 pre-eclampsia. *Placenta*. 1998;19:581-6.
362 11. D'Souza V, Rani A, Patil V, Pisal H, Randhir K, Mehendale S, Wagh G, Gupte S and Joshi S.
363 Increased oxidative stress from early pregnancy in women who develop preeclampsia. *Clin Exp*
364 *Hypertens*. 2016;38:225-32.
365 12. Vishnyakova PA, Volodina MA, Tarasova NV, Marey MV, Tsvirkun DV, Vavina OV,
366 Khodzhaeva ZS, Kan NE, Menon R, Vysokikh MY and Sukhikh GT. Mitochondrial role in adaptive
367 response to stress conditions in preeclampsia. *Sci Rep*. 2016;6:32410.
368 13. Salgado SS and Salgado MKR. Structural changes in pre-eclamptic and eclamptic
369 placentas--an ultrastructural study. *J Coll Physicians Surg Pak*. 2011;21:482-6.
370 14. Janani C and Ranjitha Kumari BD. PPAR gamma gene--a review. *Diabetes Metab Syndr*.
371 2015;9:46-50.
372 15. Corona JC and Duchen MR. PPARgamma as a therapeutic target to rescue mitochondrial
373 function in neurological disease. *Free Radic Biol Med*. 2016;100:153-163.
374 16. Barak Y, Nelson MC, Ong ES, Jones YZ, Ruiz-Lozano P, Chien KR, Koder A and Evans RM.
375 PPAR gamma is required for placental, cardiac, and adipose tissue development. *Mol Cell*.
376 1999;4:585-95.
377 17. Barak Y, Liao D, He W, Ong ES, Nelson MC, Olefsky JM, Boland R and Evans RM. Effects of
378 peroxisome proliferator-activated receptor delta on placentation, adiposity, and colorectal cancer.
379 *Proc Natl Acad Sci U S A*. 2002;99:303-8.
380 18. Schaiff WT, Carlson MG, Smith SD, Levy R, Nelson DM and Sadovsky Y. Peroxisome
381 proliferator-activated receptor-gamma modulates differentiation of human trophoblast in a
382 ligand-specific manner. *J Clin Endocrinol Metab*. 2000;85:3874-81.
383 19. Waite LL, Louie RE and Taylor RN. Circulating activators of peroxisome proliferator-activated

384 receptors are reduced in preeclamptic pregnancy. *J Clin Endocrinol Metab*. 2005;90:620-6.
385 20. Waite LL, Person EC, Zhou Y, Lim KH, Scanlan TS and Taylor RN. Placental peroxisome
386 proliferator-activated receptor-gamma is up-regulated by pregnancy serum. *J Clin Endocrinol*
387 *Metab*. 2000;85:3808-14.
388 21. McCarthy FP, Drewlo S, Kingdom J, Johns EJ, Walsh SK and Kenny LC. Peroxisome
389 proliferator-activated receptor-gamma as a potential therapeutic target in the treatment of
390 preeclampsia. *Hypertension*. 2011;58:280-6.
391 22. Kohan-Ghadr HR, Kilburn BA, Kadam L, Johnson E, Kolb BL, Rodriguez-Kovacs J, Hertz M,
392 Armant DR and Drewlo S. Rosiglitazone augments antioxidant response in the human
393 trophoblast and prevents apoptosisdagger. *Biol Reprod*. 2019;100:479-494.
394 23. Liu B, Lin X, Yang X, Dong H, Yue X, Andrade KC, Guo Z, Yang J, Wu L, Zhu X, Zhang S, Tian
395 D, Wang J, Cai Q, Chen Q, Mao S, Chen Q and Chang J. Downregulation of RND3/RhoE in
396 glioblastoma patients promotes tumorigenesis through augmentation of notch transcriptional
397 complex activity. *Cancer Med*. 2015;4:1404-16.
398 24. Yue X, Yang X, Lin X, Yang T, Yi X, Dai Y, Guo J, Li T, Shi J, Wei L, Fan GC, Chen C and Chang J.
399 Rnd3 haploinsufficient mice are predisposed to hemodynamic stress and develop apoptotic
400 cardiomyopathy with heart failure. *Cell Death Dis*. 2014;5:e1284.
401 25. Yue X, Lin X, Yang T, Yang X, Yi X, Jiang X, Li X, Li T, Guo J, Dai Y, Shi J, Wei L, Youker KA,
402 Torre-Amione G, Yu Y, Andrade KC and Chang J. Rnd3/RhoE Modulates Hypoxia-Inducible
403 Factor 1alpha/Vascular Endothelial Growth Factor Signaling by Stabilizing Hypoxia-Inducible
404 Factor 1alpha and Regulates Responsive Cardiac Angiogenesis. *Hypertension*. 2016;67:597-605.
405 26. Yang X, Wang T, Lin X, Yue X, Wang Q, Wang G, Fu Q, Ai X, Chiang DY, Miyake CY, Wehrens
406 XHT and Chang J. Genetic deletion of Rnd3/RhoE results in mouse heart calcium leakage through
407 upregulation of protein kinase A signaling. *Circ Res*. 2015;116:e1-e10.
408 27. Dai Y, Song J, Li W, Yang T, Yue X, Lin X, Yang X, Luo W, Guo J, Wang X, Lai S, Andrade KC
409 and Chang J. RhoE Fine-Tunes Inflammatory Response in Myocardial Infarction. *Circulation*.
410 2019;139:1185-1198.
411 28. Lin X, Liu B, Yang X, Yue X, Diao L, Wang J and Chang J. Genetic deletion of Rnd3 results in
412 aqueductal stenosis leading to hydrocephalus through up-regulation of Notch signaling. *Proc*
413 *Natl Acad Sci U S A*. 2013;110:8236-41.
414 29. Moses E, Johnson M, East C, Dyer T, Roten L, Proffitt J, Fenstad M, Aalto-Viljakainen T,
415 Makikallio K, Heinonen S, Kajantie E, Kere J, Laivuori H, Austgulen R, Blangero J and Brennecke S.
416 OS077. The chromosome 2q22 preeclampsia susceptibility locus reveals shared novel risk factors
417 for CVD. *Pregnancy Hypertens*. 2012;2:219-20.
418 30. Xu Y, Wu D, Liu J, Huang S, Zuo Q, Xia X, Jiang Y, Wang S, Chen Y, Wang T and Sun L.
419 Downregulated lncRNA HOXA11-AS Affects Trophoblast Cell Proliferation and Migration by
420 Regulating RND3 and HOXA7 Expression in PE. *Mol Ther Nucleic Acids*. 2018;12:195-206.
421 31. Xu Y, Ge Z, Zhang E, Zuo Q, Huang S, Yang N, Wu D, Zhang Y, Chen Y, Xu H, Huang H, Jiang
422 Z and Sun L. The lncRNA TUG1 modulates proliferation in trophoblast cells via epigenetic
423 suppression of RND3. *Cell Death Dis*. 2017;8:e3104.
424 32. Fang YN, Huang ZL, Li H, Tan WB, Zhang QG, Wang L and Wu JL. Highly expressed
425 miR-182-5p can promote preeclampsia progression by degrading RND3 and inhibiting
426 HTR-8/SVneo cell invasion. *Eur Rev Med Pharmacol Sci*. 2018;22:6583-6590.
427 33. Medvedev AV, Snedden SK, Raimbault S, Ricquier D and Collins S. Transcriptional regulation

428 of the mouse uncoupling protein-2 gene. Double E-box motif is required for peroxisome
429 proliferator-activated receptor-gamma-dependent activation. *The Journal of biological*
430 *chemistry*. 2001;276:10817-23.
431 34. Torbergsen T, Oian P, Mathiesen E and Borud O. Pre-eclampsia--a mitochondrial disease?
432 *Acta Obstet Gynecol Scand*. 1989;68:145-8.
433 35. Mando C, De Palma C, Stampalija T, Anelli GM, Figus M, Novielli C, Parisi F, Clementi E,
434 Ferrazzi E and Cetin I. Placental mitochondrial content and function in intrauterine growth
435 restriction and preeclampsia. *Am J Physiol Endocrinol Metab*. 2014;306:E404-13.
436 36. Maranzana E, Barbero G, Falasca AI, Lenaz G and Genova ML. Mitochondrial respiratory
437 supercomplex association limits production of reactive oxygen species from complex I. *Antioxid*
438 *Redox Signal*. 2013;19:1469-80.
439 37. Shi Z, Long W, Zhao C, Guo X, Shen R and Ding H. Comparative proteomics analysis
440 suggests that placental mitochondria are involved in the development of pre-eclampsia. *PLoS*
441 *One*. 2013;8:e64351.
442 38. Roberts JM, Taylor RN, Musci TJ, Rodgers GM, Hubel CA and McLaughlin MK. Preeclampsia:
443 an endothelial cell disorder. *Am J Obstet Gynecol*. 1989;161:1200-4.
444 39. Doridot L, Chatre L, Ducat A, Vilotte JL, Lombes A, Mehats C, Barbaux S, Calicchio R, Ricchetti
445 M and Vaiman D. Nitroso-redox balance and mitochondrial homeostasis are regulated by STOX1,
446 a pre-eclampsia-associated gene. *Antioxid Redox Signal*. 2014;21:819-34.
447 40. Lartey J, Gampel A, Pawade J, Mellor H and Bernal AL. Expression of RND proteins in human
448 myometrium. *Biol Reprod*. 2006;75:452-61.
449 41. Kim YS, Hori M, Yasuda K and Ozaki H. Differences in the gestational pattern of mRNA
450 expression of the Rnd family in rat and human myometria. *Comp Biochem Physiol A Mol Integr*
451 *Physiol*. 2005;142:410-5.
452 42. Cario-Toumaniantz C, Reillaudoux G, Sauzeau V, Heutte F, Vaillant N, Finet M, Chardin P,
453 Loirand G and Pacaud P. Modulation of RhoA-Rho kinase-mediated Ca2+ sensitization of rabbit
454 myometrium during pregnancy - role of Rnd3. *J Physiol*. 2003;552:403-13.
455 43. Ho PW, Liu HF, Ho JW, Zhang WY, Chu AC, Kwok KH, Ge X, Chan KH, Ramsden DB and Ho
456 SL. Mitochondrial uncoupling protein-2 (UCP2) mediates leptin protection against MPP+ toxicity
457 in neuronal cells. *Neurotox Res*. 2010;17:332-43.
458 44. Arsenijevic D, Onuma H, Pecqueur C, Raimbault S, Manning BS, Miroux B, Couplan E,
459 Alves-Guerra MC, Goubern M, Surwit R, Bouillaud F, Richard D, Collins S and Ricquier D.
460 Disruption of the uncoupling protein-2 gene in mice reveals a role in immunity and reactive
461 oxygen species production. *Nat Genet*. 2000;26:435-9.
462 45. Casteilla L, Rigoulet M and Penicaud L. Mitochondrial ROS metabolism: modulation by
463 uncoupling proteins. *IUBMB Life*. 2001;52:181-8.
464 46. Jezek P and Garlid KD. Mammalian mitochondrial uncoupling proteins. *Int J Biochem Cell*
465 *Biol*. 1998;30:1163-8.
466 47. Cadenas S. Mitochondrial uncoupling, ROS generation and cardioprotection. *Biochim*
467 *Biophys Acta Bioenerg*. 2018;1859:940-950.
468 48. Negre-Salvayre A, Hirtz C, Carrera G, Cazenave R, Troly M, Salvayre R, Penicaud L and
469 Casteilla L. A role for uncoupling protein-2 as a regulator of mitochondrial hydrogen peroxide
470 generation. *FASEB J*. 1997;11:809-15.
471 49. Pi J, Bai Y, Daniel KW, Liu D, Lyght O, Edelstein D, Brownlee M, Corkey BE and Collins S.

Persistent oxidative stress due to absence of uncoupling protein 2 associated with impaired pancreatic beta-cell function. *Endocrinology*. 2009;150:3040-8.
50. Ding Y, Zheng Y, Huang J, Peng W, Chen X, Kang X and Zeng Q. UCP2 ameliorates mitochondrial dysfunction, inflammation, and oxidative stress in lipopolysaccharide-induced acute kidney injury. *Int Immunopharmacol*. 2019;71:336-349.
51. Peng W, Huang J, Zheng Y, Ding Y, Li S, Zhang J, Lyu J and Zeng Q. UCP2 silencing aggravates mitochondrial dysfunction in astrocytes under septic conditions. *Mol Med Rep*. 2019;20:4459-4466.
52. Kalani K, Yan SF and Yan SS. Mitochondrial permeability transition pore: a potential drug target for neurodegeneration. *Drug Discov Today*. 2018;23:1983-1989.
53. Zorova LD, Popkov VA, Plotnikov EY, Silachev DN, Pevzner IB, Jankauskas SS, Babenko VA, Zorov SD, Balakireva AV, Juhaszova M, Sollott SJ and Zorov DB. Mitochondrial membrane potential. *Anal Biochem*. 2018;552:50-59.
54. Villarroya F, Iglesias R and Giralt M. PPARs in the Control of Uncoupling Proteins Gene Expression. *PPAR Res*. 2007;2007:74364.
55. Kelly LJ, Vicario PP, Thompson GM, Candelore MR, Doebber TW, Ventre J, Wu MS, Meurer R, Forrest MJ, Conner MW, Cascieri MA and Moller DE. Peroxisome proliferator-activated receptors gamma and alpha mediate in vivo regulation of uncoupling protein (UCP-1, UCP-2, UCP-3) gene expression. *Endocrinology*. 1998;139:4920-7.
56. Digby JE, Crowley VE, Sewter CP, Whitehead JP, Prins JB and O'Rahilly S. Depot-related and thiazolidinedione-responsive expression of uncoupling protein 2 (UCP2) in human adipocytes. *Int J Obes Relat Metab Disord*. 2000;24:585-92.
57. Yiallourides M, Sebert SP, Wilson V, Sharkey D, Rhind SM, Symonds ME and Budge H. The differential effects of the timing of maternal nutrient restriction in the ovine placenta on glucocorticoid sensitivity, uncoupling protein 2, peroxisome proliferator-activated receptor-gamma and cell proliferation. *Reproduction*. 2009;138:601-8.

Figure 1. The expression of RND3 is downregulated in human placentae with PE. (**A**) Representative RND3 protein expression by Western blot analysis. Densitometry of bands was performed by Image J. (**B**) Relative levels of *Rnd3* mRNA from 34 human normal term placentae and 24 human placentae with PE.

515
516 **Figure 2. Decreased RND3 expression levels are associated with severe oxidative**
517 **stress and apoptosis in PE patient derived-human primary trophoblasts.** (**A**)
518 Severe oxidative stress was observed in human placental tissue sections from PE
519 patients by DHE staining. The nuclei were visualized by blue DAPI staining. Scale
520 bar represents 200 μm. (**B**) Isolated human primary trophoblast cells (PTBs) were
521 identified by the cell surface marker CK7 shown in red and the nuclei were visualized
522 by DAPI. The purity of primary trophoblasts was calculated by the ratio of
523 CK7-positive cells over nuclei. The scale bar represents 50 μm. (**C**) RND3 protein
524 expression in PTBs was labeled by immunostaining. Decreased RND3 expression
525 along with increased ROS levels were observed in the PTBs from PE patients. The
526 scale bar represents 5 μm. (**D**) Elevated ROS levels and severe apoptosis were
527 observed in the PE PTBs compared with those of the PTBs from healthy control
528 subjects. ROS was labeled by DHE staining shown in red. The arrows point at the
529 TUNEL-positive cells (green), which overlapped with nuclear counter-staining (blue).
530 The scale bar represents 40 μm.
531
532 **Figure 3. Abnormal mitochondria were observed in the human placental**
533 **trophoblasts with PE.** (**A**) Placental tissues from PE patients and healthy control
534 subjects were analyzed by transmission electron microscopy and viewed at a low
535 magnification (upper panel) and a high magnification (lower panel), respectively. The
536 arrows point at the damaged mitochondria. The scale bars represent 1 μm and 0.5 μm,
537 respectively. (**B**) Mitochondrial membrane potentials were shown by the JC1 staining
538 of the primary trophoblast cells isolated from PE patients and healthy control subjects
539 with or without hypoxic cell culture. JC1 is a cell permeable dye that accumulates in
540 mitochondria and yields green fluorescence. Driven by high mitochondrial membrane
541 potential, JC1 is able to enter the mitochondrial inner membrane and yield red
542 fluorescence. The ratios of the red/green fluorescence intensities were quantified by
543 the image J software. The numbers in the columns represent the numbers of cells in
544 each group. C-PTBs indicates control-primary trophoblasts, and P-PTBs indicates
545 PE-primary trophoblasts.
546
547 **Figure 4. RND3 represses the hypoxia-induced ROS generation and apoptosis in**
548 **trophoblastic BeWo cells.** (**A**) Reduced ROS levels were observed in hypoxic
549 conditions and were challenged with GFP-Rnd3 overexpressing BeWo cells. ROS was
550 labeled by DHE staining shown in red. The arrows point at the GFP-Rnd3 expressing
551 cells. The scale bar represents 80 μm. (**B**) A decrease in 8-isoprostane levels was
552 detected in the cell lysates of myc-Rnd3 overexpressing BeWo cells, compared with
553 those noted in the myc control group. The experiments were repeated 3 times. (**C**) The
554 comparison of the TUNEL staining in myc and myc-Rnd3 overexpressing BeWo cells
555 following 16 h of hypoxic cell culture. The arrows indicate TUNEL-positive cells
556 (green) overlapping with nuclear counter-staining. The scale bar represents 200 μm.
557 (**D**) Quantification of TUNEL-positive cells. The experiments were repeated 3 times.
558

559 **Figure 5. RND3 deficiency results in mitochondrial dysfunction.** (**A**) By
560 transmission electron microscope analysis, mitochondrial damage was observed in
561 siRnd3 transiently transfected BeWo cells. The arrow heads indicate the loss of crista
562 in the damaged mitochondria. The images of a series of magnifications are displayed.
563 (**B**) The depolarized mitochondrial membrane potential was detected in siRnd3
564 transfected BeWo cells compared with that noted in the siCtrl group. The
565 mitochondrial membrane potential was quantified by the ratios of red/green
566 fluorescence intensities of mitochondria-specific JC1 dye. (**C**) The Oxygen
567 consumption rate (OCR) of treated BeWo cells was measured prior to and following
568 the injections of oligomycin, FCCP, rotenone and antimycin A (Rot/AA), respectively.
569 Increased proton leak was detected in the siRnd3 group. (**D**) Reduced coupler
570 efficiency was detected in siRnd3 transfected BeWo cells compared with that noted in
571 the siCtrl group as determined by mitochondrial OCR determination. The scale bar
572 represents 80 μm. The numbers in the columns represent the number of cells in each
573 group.

574

575 **Figure 6. RND3 interacts with PPARγ and promotes the PPARγ-UCP2 cascade.**
576 (**A**) Increased expression levels of UCP2 and PPARγ were observed following RND3
577 overexpression. (**B**) Knockdown of RND3 results in lower UCP2 and PPARγ protein
578 expression levels. (**C**) Q-PCR analysis indicated that *UCP2* mRNA levels were
579 increased in myc-Rnd3 expressed cells, whereas they were reduced in RND3 deficient
580 cells. (**D**) Nuclear protein levels of RND3 and PPARγ were increased in the
581 myc-Rnd3 overexpressed cells and were decreased in the RND3 deficient cells. (**E**)
582 RND3 regulated PPARγ transcriptional activity as demonstrated by luciferase assays.
583 (**F**) Myc-Rnd3 physically interacted with flag-PPARγ *in vivo* as determined by
584 coimmunoprecipitation. (**G**) Immunofluorescence staining indicated the
585 co-localization of PPARγ and RND3 proteins. Knockdown of RND3 reduced the
586 nuclear accumulation of the PPARγ protein. The scale bar represents 100 μm.
587

588 **Figure 7. RND3 deficiency-mediated oxidative stress and mitochondrial**
589 **dysfunction are attenuated by PPARγ overexpression.** (**A**) JC1 staining was
590 performed in BeWo cells among the three following groups: siCtrl, siRnd3 and
591 siRnd3 plus flag-PPARγ. The depolarization of the mitochondrial membrane potential
592 caused by RND3 knockdown was attenuated by flag-PPARγ overexpression. The
593 scale bar represents 80 μm. (**B**) The quantification of the ratios of red/green
594 fluorescence intensities. The experiments were repeated 3 times. (**C**) Transmission
595 electron microscope analysis indicates that the RND3 deficiency-induced
596 mitochondrial damage was recovered by flag-PPARγ overexpression. The arrow
597 heads display damaged mitochondrial structure in the siRnd3 group. The scale bar
598 represents 0.5 μm. (**D**) DHE staining indicates ROS levels among the three groups.
599 The scale bar represents 100 μm. (**E**) The ROS levels were quantified by the
600 densitometry of DHE staining. The experiments were repeated 3 times. (**F**)
601 8-isoprostane levels were detected in the cell lysates of the three groups. (**G**) Q-PCR

602 analysis of *UCP2* mRNA levels among the three groups. The experiments were
603 repeated 3 times. (**H**) Immunoblots revealed increased UCP2 protein expression
604 levels in the flag-PPARγ rescue group. (**I**) Mitochondrial respiratory function was
605 measured. The proton leak associated OCR was improved by PPARγ. (**J**) RND3
606 deficiency-mediated defective coupler efficiency was ameliorated by PPARγ.
607
608 **Figure 8. Oxidative stress and mitochondrial dysfunction in PE patient-derived**
609 **PTBs are partially rescued by RND3 overexpression. (A**) Human PTBs from PE
610 patient and healthy control subjects were infected with Ad-GFP-hRND3. Hypoxic cell
611 culture was applied to induce oxidative stress. The arrow heads represent the
612 GFP-RND3 expressing PTBs (green fluorescence). The long arrows represent the
613 PTBs with non-GFP-RND3. ROS levels were significantly reduced in PE-PTBs
614 following GFP-RND3 overexpression as determined by DHE staining. NS indicates
615 non-specific staining. The scale bar represents 25 μm. (**B**) 8-isoprostane level
616 detection in the C-PTBs and P-PTBs following treatment of Ad-GFP or
617 Ad-GFP-Rnd3. (**C**) Ad-GFP-hRND3 improved *UCP2* mRNA transcripts in the PTBs.
618 (**D**) RND3 overexpression rescued PPARγ-UCP2 signaling in PE-PTBs.
619 Mitochondrial dysfunction in PE-PTBs was partially rescued by Ad-GFP-hRND3, as
620 determined by the increases in proton leak associated OCR (**E**) and respiratory control
621 ratio (**F**). C-PTBs indicates control-primary trophoblasts; P-PTBs, PE-primary
622 trophoblasts.
623
624 **Figure 9. The downregulation of the PPARγ-UCP2 cascade is confirmed in**
625 **human placentae with PE. (A)** Representative protein expression levels of PPARγ
626 and UCP2 as determined by western blot analysis. The levels of the two proteins were
627 downregulated in the PE placentas. (**B**) Relative mRNA levels of *PPARγ* from 34
628 normal term placentae and 24 PE placentae. (**C**) Relative mRNA levels of *UCP2* from
629 34 normal term placentae and 24 PE placentae.
630

Figure 1

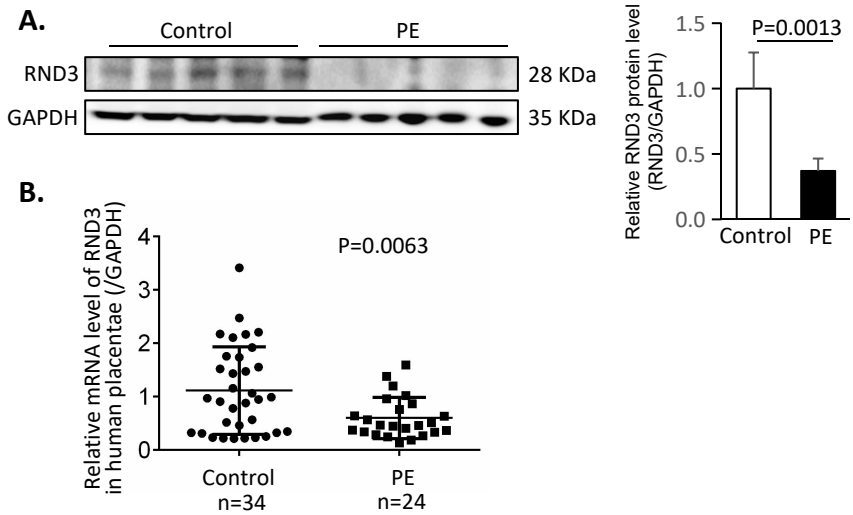
A.
Control
PE
RND3
GAPDH
28 KDa
35 KDa
Relative RND3 protein level (RND3/GAPDH)
1.5
1.0
0.5
0.0
P=0.0013
Control
PE
B.
Relative mRNA level of RND3 in human placentae (/GAPDH)
4
3
2
1
0
P=0.0063
Control n=34
PE n=24

Figure 2

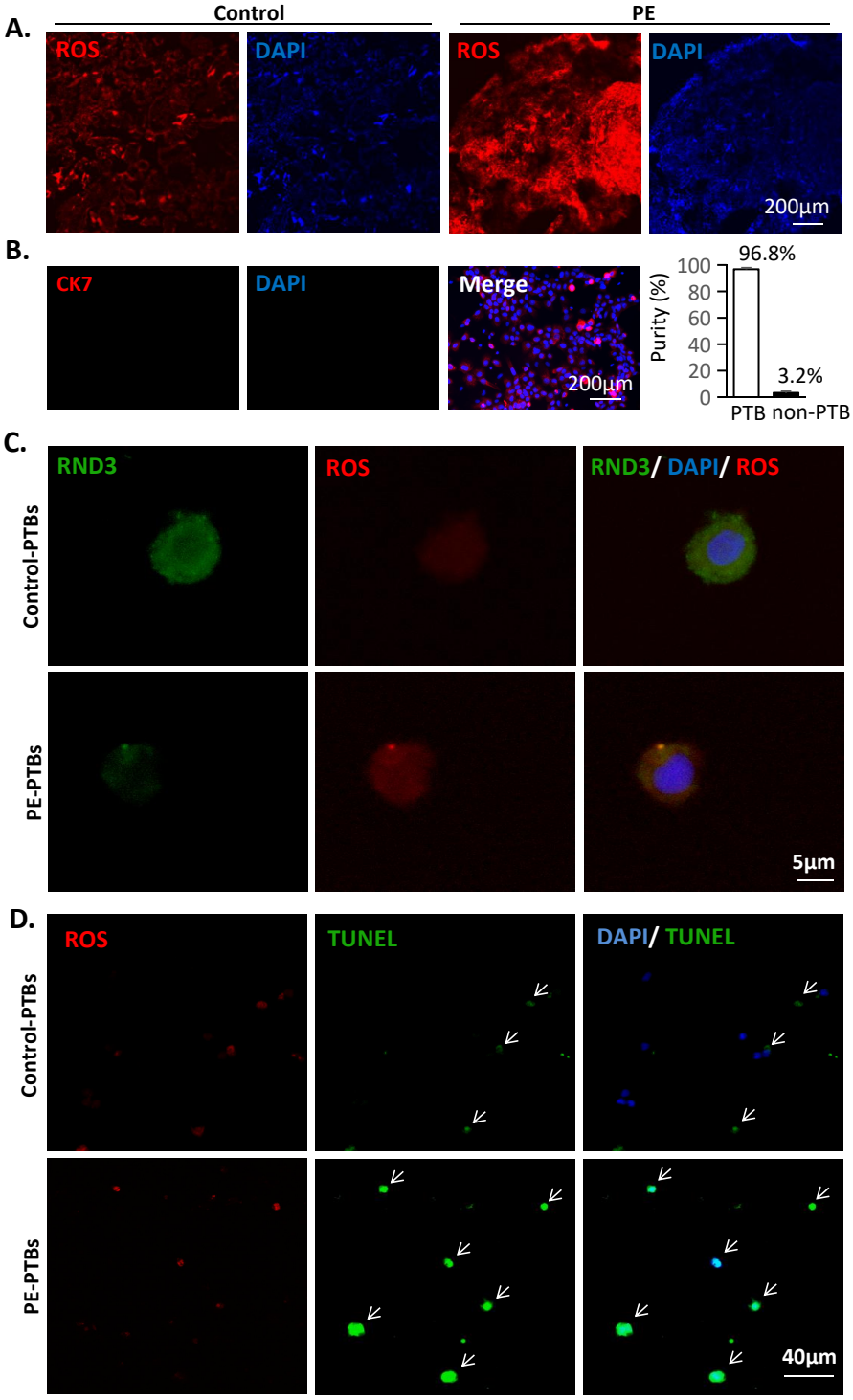
A.
Control
PE
ROS
DAPI
ROS
DAPI
200μm
B.
CK7
DAPI
Merge
200μm
Purity (%)
100
80
60
40
20
0
96.8%
3.2%
PTB
non-PTB
C.
Control-PTBs
PE-PTBs
RND3
ROS
RND3/ DAPI/ ROS
5μm
D.
Control-PTBs
PE-PTBs
ROS
TUNEL
DAPI/ TUNEL
40μm

Figure 3

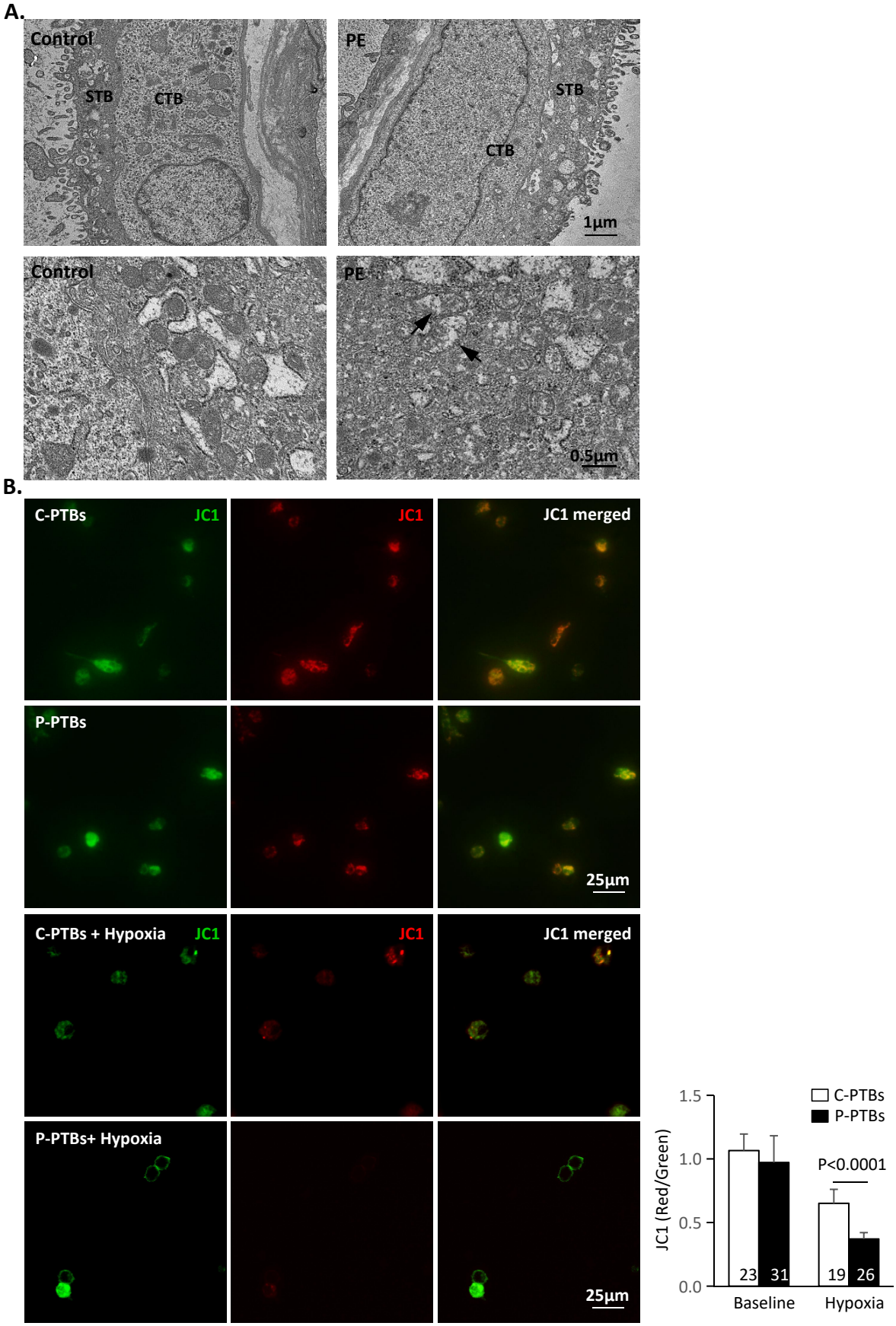
A.
Control
STB
CTB
PE
STB
CTB
1µm
Control
PE
0.5µm
B.
C-PTBs
JC1
JC1
JC1 merged
P-PTBs
25µm
C-PTBs + Hypoxia
JC1
JC1
JC1 merged
P-PTBs+ Hypoxia
25µm
C-PTBs
P-PTBs
JC1 (Red/Green)
1.5
1.0
0.5
0.0
P<0.0001
23
31
19
26
Baseline
Hypoxia

Figure 4

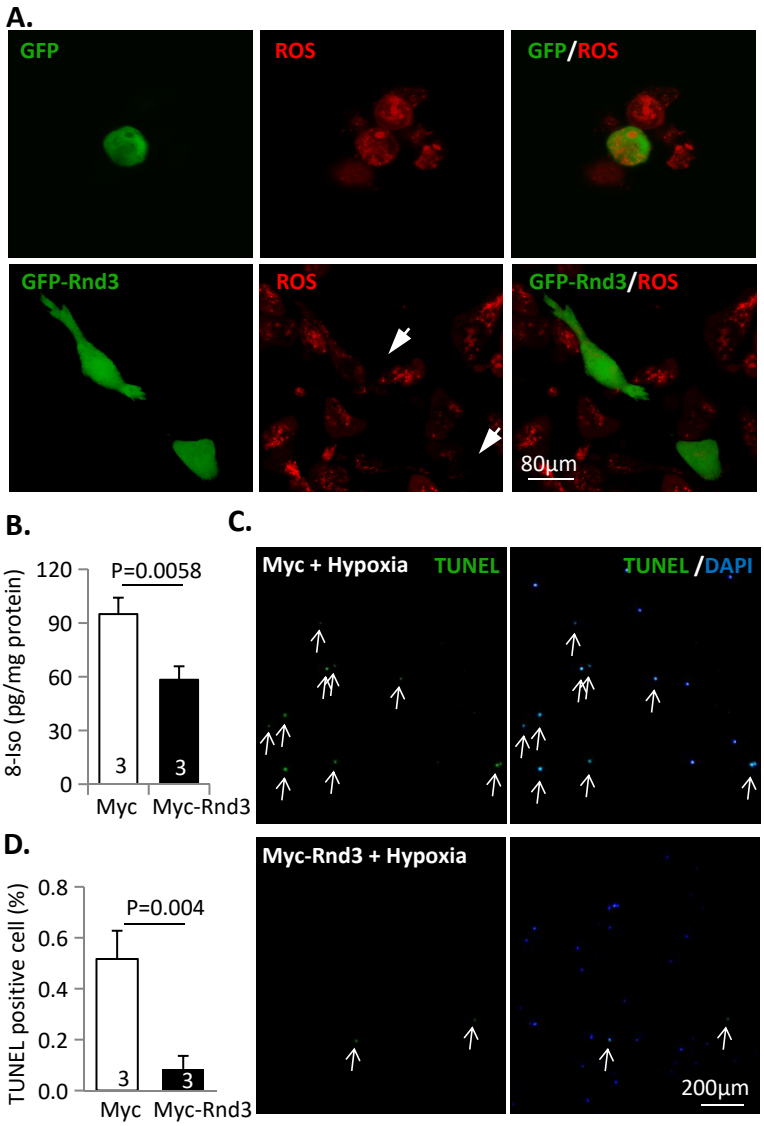
A.
GFP
ROS
GFP/ROS
GFP-Rnd3
ROS
GFP-Rnd3/ROS
80μm
B.
8-Iso (pg/mg protein)
120
90
60
30
0
P=0.0058
3
3
Myc
Myc-Rnd3
C.
Myc + Hypoxia
TUNEL
TUNEL /DAPI
Myc-Rnd3 + Hypoxia
200μm
D.
TUNEL positive cell (%)
0.8
0.6
0.4
0.2
0.0
P=0.004
3
3
Myc
Myc-Rnd3

Figure 5

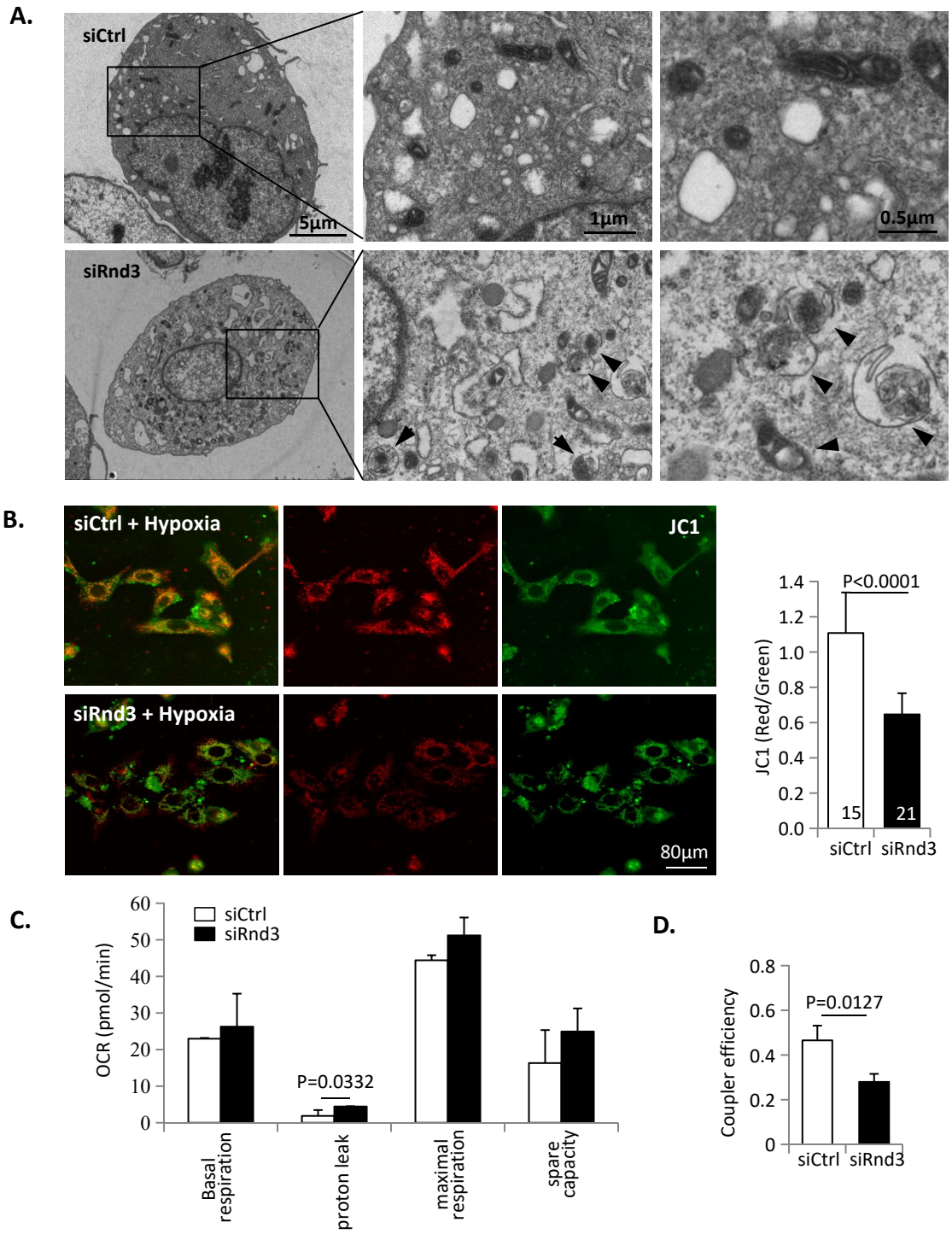
A.
siCtrl
5µm
1µm
0.5µm
siRnd3
B.
siCtrl + Hypoxia
JC1
siRnd3 + Hypoxia
80µm
P<0.0001
JC1 (Red/Green)
1.4
1.2
1.0
0.8
0.6
0.4
0.2
0.0
15
21
siCtrl
siRnd3
C.
siCtrl
siRnd3
OCR (pmol/min)
60
50
40
30
20
10
0
P=0.0332
Basal respiration
proton leak
maximal respiration
spare capacity
D.
Coupler efficiency
0.8
0.6
0.4
0.2
0
P=0.0127
siCtrl
siRnd3

Figure 6

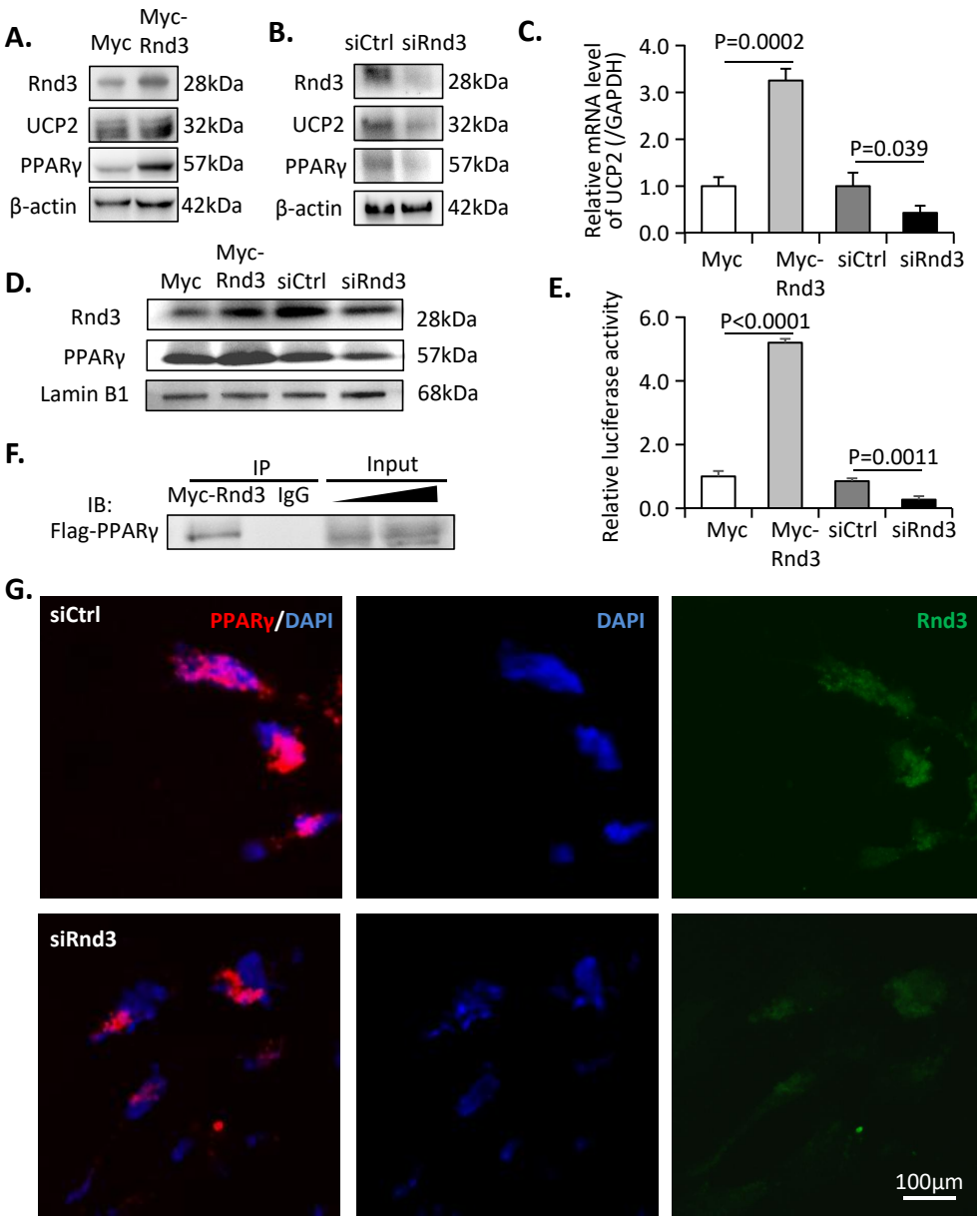
A.
Myc
Myc-Rnd3
Rnd3
UCP2
PPARγ
β-actin
28kDa
32kDa
57kDa
42kDa
B.
siCtrl
siRnd3
Rnd3
UCP2
PPARγ
β-actin
28kDa
32kDa
57kDa
42kDa
C.
Relative mRNA level of UCP2 (/GAPDH)
4.0
3.0
2.0
1.0
0.0
P=0.0002
P=0.039
Myc
Myc-Rnd3
siCtrl
siRnd3
D.
Myc
Myc-Rnd3
siCtrl
siRnd3
Rnd3
PPARγ
Lamin B1
28kDa
57kDa
68kDa
E.
Relative luciferase activity
6.0
4.0
2.0
0.0
P<0.0001
P=0.0011
Myc
Myc-Rnd3
siCtrl
siRnd3
F.
IP
Input
Myc-Rnd3
IgG
IB:
Flag-PPARγ
G.
siCtrl
PPARγ/DAPI
DAPI
Rnd3
siRnd3
100μm

Figure 7

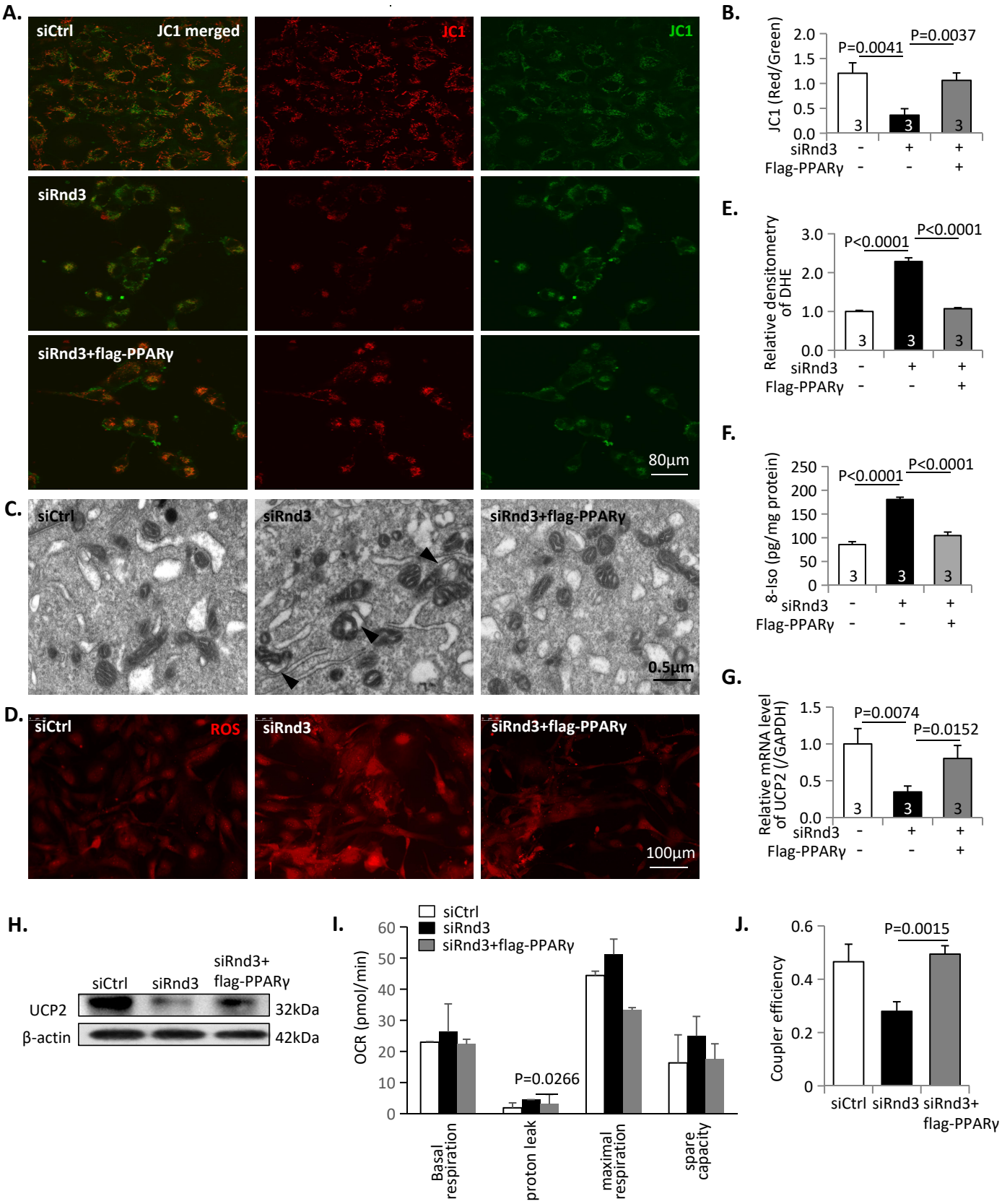
A.
siCtrl
JC1 merged
JC1
JC1
siRnd3
siRnd3+flag-PPARγ
80μm
B.
JC1 (Red/Green)
P=0.0041
P=0.0037
siRnd3
Flag-PPARγ
C.
siCtrl
siRnd3
siRnd3+flag-PPARγ
0.5μm
D.
siCtrl
ROS
siRnd3
siRnd3+flag-PPARγ
100μm
E.
Relative densitometry of DHE
P<0.0001
P<0.0001
F.
8-Iso (pg/mg protein)
P<0.0001
P<0.0001
G.
Relative mRNA level of UCP2 (/GAPDH)
P=0.0074
P=0.0152
H.
siCtrl
siRnd3
siRnd3+ flag-PPARγ
UCP2
β-actin
32kDa
42kDa
I.
siCtrl
siRnd3
siRnd3+flag-PPARγ
OCR (pmol/min)
P=0.0266
Basal respiration
proton leak
maximal respiration
spare capacity
J.
Coupler efficiency
P=0.0015
siCtrl
siRnd3
siRnd3+ flag-PPARγ

Figure 8

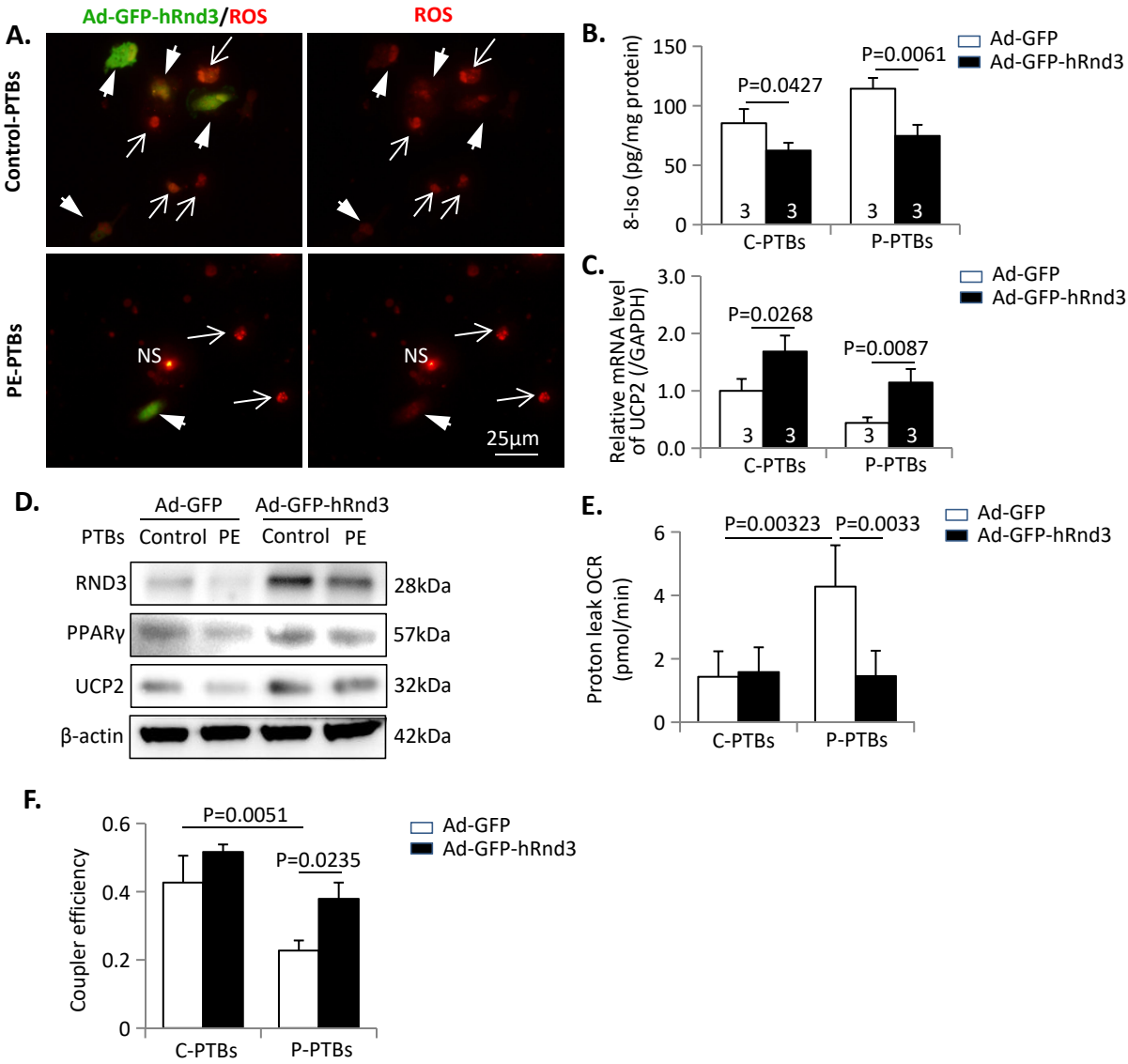
A.
Ad-GFP-hRnd3/ROS
ROS
Control-PTBs
PE-PTBs
NS
NS
25μm
B.
8-Iso (pg/mg protein)
150
100
50
0
P=0.0427
P=0.0061
3
3
3
3
C-PTBs
P-PTBs
Ad-GFP
Ad-GFP-hRnd3
C.
Relative mRNA level of UCP2 (/GAPDH)
3.0
2.0
1.0
0.0
P=0.0268
P=0.0087
3
3
3
3
C-PTBs
P-PTBs
Ad-GFP
Ad-GFP-hRnd3
D.
Ad-GFP
Ad-GFP-hRnd3
PTBs
Control
PE
Control
PE
RND3
28kDa
PPARγ
57kDa
UCP2
32kDa
β-actin
42kDa
E.
Proton leak OCR (pmol/min)
6
4
2
0
P=0.00323
P=0.0033
C-PTBs
P-PTBs
Ad-GFP
Ad-GFP-hRnd3
F.
Coupler efficiency
0.6
0.4
0.2
0
P=0.0051
P=0.0235
C-PTBs
P-PTBs
Ad-GFP
Ad-GFP-hRnd3

Figure 9

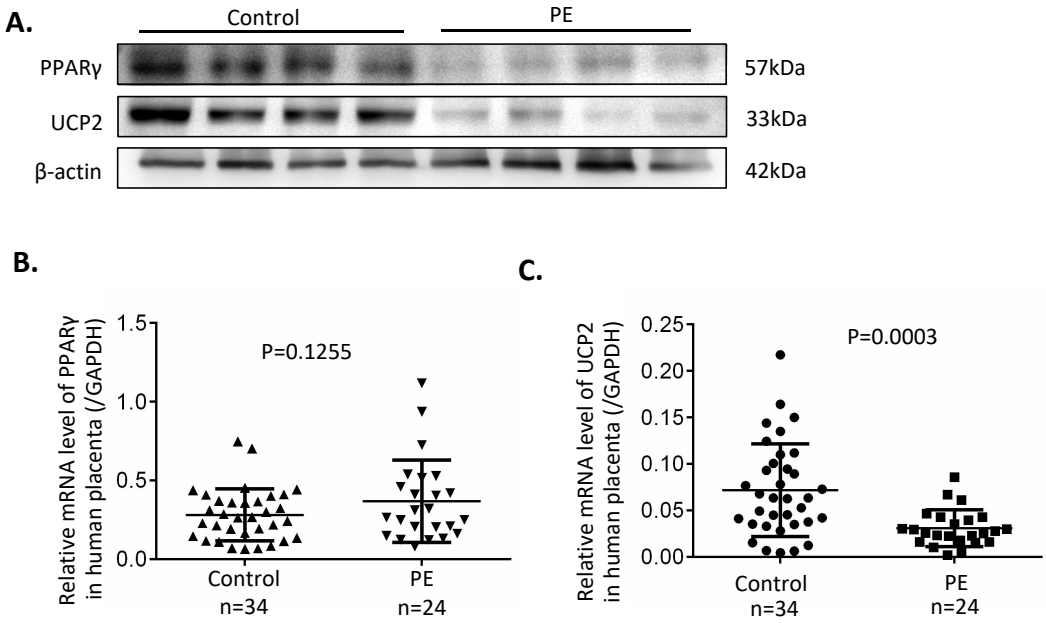
A.
Control
PE
PPARγ
UCP2
β-actin
57kDa
33kDa
42kDa
B.
Relative mRNA level of PPARγ in human placenta (/GAPDH)
1.5
1.0
0.5
0.0
P=0.1255
Control n=34
PE n=24
C.
Relative mRNA level of UCP2 in human placenta (/GAPDH)
0.25
0.20
0.15
0.10
0.05
0.00
P=0.0003
Control n=34
PE n=24